Life Sciences 239 (2019) 117010

Contents lists available at ScienceDirect

Life Sciences

journal homepage: www.elsevier.com/locate/lifescie

# Amlexanox reversed non-alcoholic fatty liver disease through IKKε inhibition of hepatic stellate cell

Qian He[a,1], Xuan Xia[b,f,1], Kecheng Yao[a], Jun Zeng[c], Wei Wang[c], Qiong Wu[d], Renmin Tang[c], Xiulan Zou[a,e,*]

[a] Department of Geriatrics, The People's Hospital of China Three Gorges University/the First People's Hospital of Yichang, Yichang, 443000, Hubei Province, China
[b] Department of Physiology and Pathophysiology, College of Medical Sciences, China Three Gorges University, Yichang, 443002, Hubei Province, China
[c] Department of Endocrinology, The People's Hospital of China Three Gorges University/the First People's Hospital of Yichang, Yichang, 443000, Hubei Province, China
[d] Department of Pediatrics, The People's Hospital of China Three Gorges University/the First People's Hospital of Yichang, Yichang, 443000, Hubei Province, China
[e] Yunji Community Healthcare Center, The People's Hospital of China Three Gorges University/the First People's Hospital of Yichang, Yichang, 443000, Hubei Province, China
[f] Third-Grade Pharmacological Laboratory on Chinese Medicine Approved By State Administration of Traditional Chinese Medicine, Medical College of China Three Gorges University, Yichang, 443002, Hubei Province, China

ARTICLE INFO

*Keywords:*
Amlexanox
IKKε
NAFLD
Hepatic stellate cell

ABSTRACT

*Aims:* Amlexanox, an inhibitor of nuclear factor κB kinase epsilon (IKKε) and TANK-binding kinase 1(TBK1), was demonstrated to be effective in diabetes and obesity. The aim of this study was to explore the molecular mechanisms of its role in non-alcoholic fatty liver disease (NAFLD).

*Main methods:* NAFLD mouse models were established by using eight-week-old male C57BL/6 mice fed with high-fat diet (HFD) or (and) lipopolysaccharide (LPS) for 18 weeks. From the beginning of HFD, HFD-induced mice were subjected to amlexanox or vehicle for 18 weeks. HFD + LPS-induced mice were treated with amlexanox or vehicle for the last 6 weeks. Blood biochemistry parameters were determined using automatic biochemistry analyzer. Histological changes of liver tissue were observed by hematoxylin-eosin (H&E) staining and Oil Red O staining. The expressions of IKKε and smooth muscle actin-α (α-SMA) were evaluated through immunohistochemistry. Serum inflammatory mediator was determined by enzyme linked immunosorbent assay (ELISA). Gene expressions involved in glucose and lipid metabolism, insulin signaling pathway were examined using quantitative RT-PCR or Western blotting.

*Key findings:* This study demonstrated that amlexanox reversed glucose and lipid metabolic disturbance and hepatic steatosis in NAFLD mice model. IKKε was specific expressed in hepatic stellate cells (HSCs) instead of hepatocytes. This study also found that amlexanox improved insulin signaling (Insulin-IRS-1-Akt) in hepatocytes through inhibiting inflammation (IKKε-NF-κB-TNF-α/IL-1α) in HSCs.

*Significance:* The present study confirmed that IKKε was specific expressed in HSCs. Inhibition of activated HSCs was responsible for effects of amlexanox on NAFLD, with improving insulin signal pathway in hepatocytes.

## 1. Introduction

Non-alcoholic fatty liver disease (NAFLD), ranging from simple steatosis to non-alcoholic steatohepatitis (NASH) [1], is the hepatic manifestation of the metabolic syndrome. NAFLD is marked with chronic low-grade inflammation accompanied by insulin resistance (IR). Hepatic insulin resistance is an important pathophysiological mechanism of glucose and lipid metabolism disorder, which is of great significance for the occurrence and development of NAFLD [2]. Insulin signaling pathways, mediated by impaired tyrosine phosphorylation of insulin receptor substrate (IRS), have previously been reported to be vital for the development of insulin resistance. Although the molecular links between inflammation and insulin resistance are not fully understood, it is clear that the nuclear factor-κB (NF-κB) pathway plays a vital role [3]. The triggering of stimulus ultimately results in nuclear translocation of NF-κB and the activation of inflammatory cascades

* Corresponding author. Department of Geriatrics and Yunji Community Healthcare Center, the People's Hospital of China Three Gorges University/the First People's Hospital of Yichang, No.4, Hudi Road, Xiling District, Yichang 443000, Hubei Province, China.
*E-mail address:* zouxl61@126.com (X. Zou).
[1] Qian He and Xuan Xia are regarded as co-first author.

https://doi.org/10.1016/j.lfs.2019.117010
Received 26 August 2019; Received in revised form 7 October 2019; Accepted 21 October 2019
Available online 28 October 2019
0024-3205/ 

**Abbreviations**

| | |
|---|---|
| AM | amlexanox |
| IKKε | inhibitor of nuclear factor κB kinase epsilon |
| TBK1 | TANK-binding kinase 1 |
| NAFLD | non-alcoholic fatty liver disease |
| NASH | non-alcoholic steatohepatitis |
| NF-κB | nuclear factor-κB |
| IR | insulin resistance |
| IRS | insulin receptor substrate |
| NC | normal chow |
| HFD | high-fat diet |
| LPS | lipopolysaccharide |
| TG | serum triglyceride |
| TC | total serum cholesterol |
| ALT | alanine aminotransferase |
| AST | aspartate transaminase |
| FFA | serum nonesterified free fatty acid |
| UCP1 | uncoupling protein 1 |
| HSCs | hepatic stellate cells |
| TNF-α | tumor necrosis factor-α |
| IL-1α | interleukin-1α |
| α-SMA | smooth muscle actin-α |
| PPAR α | peroxisome proliferator-activated receptor-α |
| FAS | fatty acid synthase |
| G6P | glucose-6-phosphase |
| PCK1 | phosphoenolpyruvate carboxykinase 1 |
| SREBP1 | sterol response element-binding protein 1 |
| CD36 | fatty acid translocase |
| PKLR | pyruvate kinase liver and red blood cell |
| CCL2 | chemokine (C–C motif) ligand 2 |
| Akt | RAC-alpha serine/threonine-protein kinase |
| CCR5 | C–C chemokine receptor type 5 |
| STAT3 | signal transducer and activator of transcription 3 |
| DAB staining | 3,3′-diaminobenzidine staining |
| H&E staining | hematoxylin-eosin staining |
| p65 | nuclear factor NF-kappa-B p65 subunit |
| qRT-PCR | quantitative real-time reverse transcriptase polymerase chain reaction |
| ELISA | enzyme linked immunosorbent assay |
| Veh | vehicle |

producing a variety of pro-inflammatory cytokines, including TNF-α and IL-6, which participate in IR via phosphorylation of insulin receptor substrate (IRS) [4]. Also, pharmacological targeting inhibition on IKKβ-NF-κB pathway could reverse diet-induced insulin resistance in liver [5].

IKKε, one of the noncanonical IKKs in NF-κB signaling, has been proved to have role in inflammatory and metabolic disease including NAFLD, type 2 diabetes, obesity, rheumatoid arthritis and tumor [6–8]. Furthermore, systemic deletion of IKKε partially restored insulin sensitivity [8]. However, studies of pharmacological interference on the pathway remain unknown.

Here we choose amlexanox (AM), previously identified as a novel chemical inhibitor of IKKε and TBK1, to observe its roles in hepatic steatosis, weight gain and insulin sensitivity. Amlexanox (also named AA-673) is artificially-synthesized pyridine-3-carboxylic acid derivative. In earlier years, amlexanox was shown to an inhibitor for immune response and leukotriene antagonist and had anti-asthma in animal model [9]. Then, amlexanox became widely-used patch to treat recurrent aphthous ulcer for decades in several nations including China [10,11]. Recently studies have reported administration of this selective TBK1 and IKKε inhibitor to obese mice significantly improves metabolic disorders, but the mechanism of amlexanox action is still completely unclear [12].

Hepatic stellate cells (HSCs), inhabiting in the Disse space between hepatocytes and sinusoidal endothelial cells, are one of the inherent nonparenchymal cell types in the liver. In the normal liver, HSCs are in a ‘quiescent’ state [13]. However, once the liver is injured, quiescent HSCs differentiate into myofibroblasts. Activated hepatic stellate cells (HSCs) are known to synthesize and secret cytokines, chemokines, extracellular matrix proteins, and other genes that contribute to liver fibrosis [14,15], but their function is poorly understood in the early stages before NAFLD fibrosis.

In the present study, we found that (i) Amlexanox reversed metabolic changes and reduced liver inflammation induced by high-fat diet (HFD) and even concurrently with lipopolysaccharide (LPS); (ii) Altered gene expression involved in glucose and lipid metabolism improved protective role of amlexanox; (iii) Amlexanox reduced IKKε expression in hepatic stellate cells; (iv) Amlexanox enhanced insulin signaling through inhibiting inflammation in HSCs. In conclusion, amlexanox was considered as a potential treatment for NAFLD through IKKε inhibition of hepatic stellate cell.

## 2. Materials and methods

### 2.1. Animals

To confirm the role of IKKε or HFD and different response to amlexanox, two mice models of non-alcoholic fatty liver were developed using eight-week-old male C57BL/6 mice fed with a high-fat diet (HFD) (60 kcal% (35 gm%), Diet: D12492; Beijing HFK Bioscience Co Ltd, China) with or without LPS injection for 18 weeks. The mice fed on normal chow diet (NC) (10 kcal% (4.3 gm%); Beijing HFK Bioscience Co Ltd, China) were contrasted with HFD group. Two mice models of NAFLD which were subjected to two independent interventions (A and B). Intervention A had three groups (n = 10 per group). Eight-week-old male C57BL/6 mice were subjected to chow diet group or 18-week HFD. From the beginning of intervention, we added vehicle (vehicle: gavage by Tris-HCl buffer) to NC (NC + Veh) and HFD group (HFD + Veh) or amlexanox (25 mg/kg, once daily, gavage, dissolved in Tris-HCl buffer) to HFD group (HFD + AM). We would compare NC + Veh and HFD + Veh, or HFD + Veh and HFD + AM in following test. Amlexanox (Abcam, St Louis) was fat soluble but easily dissolved in Tris-HCl buffer (250 mmol/L Tris-HCl buffer titrated by 150 mmol/L sodium hydroxide to pH 7.2).

Another intervention B had two groups. Eight-week-old male C57BL/6 mice were subjected to 18-week HFD + LPS (125 μg/kg, once daily, subcutaneous, saline as solvent). In the last six weeks before the end of intervention, we added vehicle (HFD + LPS + Veh) (Vehicle: gavage by Tris-HCl buffer) or amlexanox (HFD + LPS + AM) (25 mg/kg, once daily, gavage, dissolved in Tris-HCl buffer) for six-week intervention. Finally, we would compare the indicators between HFD + LPS + Veh and HFD + LPS + AM group. All the mice would be sacrificed by anesthesia. Animal studies were reported in compliance with the ARRIVE guidelines [16] and carried out in accordance with the National Institutes of Health guide for the care and use of Laboratory animals (NIH Publications No. 8023, revised 1978). All studies were conducted with the approved protocols by the animal care and ethics committee of China Three Gorges University. C57BL/6 mice, purchased from Hubei Research Center of Laboratory Animals, were housed on a 12-h light/black cycle under controlled temperature in China Three Gorges University Research Animal Center.

### 2.2. Energy balance analysis

Energy balance analysis (diet intake and bodyweight) was monitored in individual mouse using metabolic cage (Sans Biotechnology Co Ltd, China). Mice were placed in metabolic cages for 24 h before measurement. The data were collected at the indicated time for consecutive 3 days.

### 2.3. Blood biochemistry

Blood glucose was determined in the tail vein blood using portable glucometer (Roche, Basel, Switzerland). In the end of intervention, mice were anesthetized by inhaling diethyl ether in anesthesia chamber. Then we performed the orbital sinus bleeding by removing the whole eye ball. Blood were collected for checking serum triglyceride (TG), total serum cholesterol (TC), alanine aminotransferase (ALT) and aspartate transaminase (AST) by using automatic biochemistry analyzer. Serum nonesterified free fatty acid (FFA) was measured by commercial kit (Free fatty acids assay kit, Nanjing Jiancheng Bioengineering Institute, China). Serum insulin and TNF-α were determined using enzyme linked immunosorbent assay (ELISA) kit (Millipore, Bedford, MA, USA). Homeostasis model insulin resistance index was calculated as follows: homeostasis model insulin resistance assessment (HOMA-IR) = [FBG (mmol/L) × FINS (mIU/L)]/22.5.

### 2.4. Glucose tolerance test

Oral glucose tolerance test (OGTT) was performed 48 h after the indicated time and fast for 12 h followed by oral glucose gavage (2.0 g/kg body weight). Blood glucose from tail veil was measured at 0, 60, 120 and 180 min after glucose stimulation.

### 2.5. Immunoblotting assay

To determine the expression levels of selected proteins, fresh liver tissue was collected, cut into pieces, snap frozen by lipid nitrogen. 30 mg liver tissue was weighted and grinded with 1 ml Roth lysis buffer. Roth lysis buffer was comprised of 50 mM HEPES, 150 mM NaCl, 1% Triton X-100, 5 mM EDTA, 5 mM EGTA, 20 mM NaF, 10 M NaOH or HCl adjusted to pH = 7.4 and temporarily added PMSF (1 mM,100 × ,Sigma,USA), Protein phosphatase inhibitor (PPI, 100 × , Beijing Applygen Technologies Inc) when it was used. Liver tissue was grinded with Roth lysis buffer, ultrasonicated, centrifugated under 4 °C, 8000 g for 5min. Supernatant was drew into new tube and tested for protein concentration by BCA assay. 30 μg of liver protein was separated by way of 10% sodium dodecyl sulfate-polyacrylamide gel electrophoresis, then transferred onto nitrocellulose membrane and blotted with specific primary antibody. The band intensity was quantified by Odyssey Software (Odyssey CLX, LICOR Biosciences, USA). Protein expression levels were quantified by software Image J (version 1.42). All data were normalized to the control value.

### 2.6. RNA isolation and quantitative real-time reverse transcriptase polymerase chain reaction (qRT-PCR)

This study determined gene expression on hepatic gluconeogenesis genes (glucose-6-phosphase (G6P), phosphoenolpyruvate carboxykinase 1 (PCK1)), hepatic glycolysis (pyruvate kinase, liver and red blood cell (PKLR)), lipid synthesis (fatty acid synthase (FAS), sterol response element-binding protein 1 (SREBP1)), lipid oxidation (peroxisome proliferator-activated receptor-α (PPARα)), lipid transports (fatty acid translocase (CD36)), cytokine and chemokine (interleukin-1α (IL-1α), chemokine (C–C motif) ligand 2 (CCL2)) by qRT-PCR. Total RNA was extracted from frozen liver tissues (−80 °C) using the TRIzol RNA isolation reagent (Invitrogen, California). Reverse transcription of 1.0 μg RNA was executed according to the instructions of PrimeScript™ 1st Strand cDNA Synthesis Kit (RR047A, TaKaRa, Japan). The qRT-PCR reaction was done in 20 μl (SYBR® Premix Ex Taq™ RR420A, TaKaRa Japan). The results were normalized against 18s rRNA signal. The designed primers for IKKε, G6P, PCK1, FAS, SREBP1, PPARα, CD36, PKLR, IL-1α, CCL2 and 18s (control for normalization) are shown in Table 1.

**Table 1**
Primers designed for qRT-PCR.

| Oligo name | Sense | Sequence (5′-3′) | product Size (bp) |
|---|---|---|---|
| IKKε | IKKε-FWD | ACCACTAACTACCTGTGGCAT | 209 |
| | IKKε-REV | ACTGCGAATAGCTTCACGATG | |
| G6P | G6P-FWD | AGGAAGGATGGAGGAAGGAA | 162 |
| | G6P-REV | TGGAACCAGATGGGAAAGAG | |
| PCK1 | PCK1-FWD | ATCTTTGGTGGCCGTAGACCT | 179 |
| | PCK1-REV | CCGAAGTTGTAGCCGAAGAA | |
| FAS | FAS-FWD | GCCATGCCCAGAGGGTGGTT | 131 |
| | FAS-REV | AGGGTCGACCTGGTCCTCA | |
| SREBP1 | SREBP1-FWD | GAAGCTGTCGGGGTAGCGTC | 196 |
| | SREBP1-REV | CTCTCAGGAGAGTTGGCACCTG | |
| PPARα | PPARα-FWD | AACATCGAGTGTCGAATATGTGG | 101 |
| | PPARα-REV | AGCCGAATAGTTCGCCGAAAG | |
| CD36 | CD36-FWD | ATGGGCTGTGATCGGAACTG | 110 |
| | CD36-REV | GTCTTCCCAATAAGCATGTCTCC | |
| KPLR | KPLR-FWD | TCAAGGCAGGGATGAACATTG | 131 |
| | KPLR-REV | CACGGGTCTGTAGCTGAGTG | |
| IL-1α | IL-1α-FWD | AGTATCAGCAACGTCAAGCAA | 105 |
| | IL-1α- REV | TCCAGATCATGGGTTATGGACTG | |
| CCL2 | CCL2-FWD | TTAAAAACCTGGATCGGAACCAA | 121 |
| | CCL2- REV | GCATTAGCTTCAGATTTACGGGT | |
| 18s | 18s-FWD | GAAACGGCTACCACATCCAAGG | 158 |
| | 18s-REV | GCCCTCCAATGGATCCTCGTTA | |

### 2.7. Histology and morphology

The murine liver samples fixed in 4% formaldehyde were prepared and embedded in paraffin. Paraffin-embedded liver tissues were sectioned (8 μm thick) and then stained with hematoxylin & eosin dye (H&E) and immunohistochemistry (3,3′-diaminobenzidine (DAB) staining. Fresh liver was rapidly frozen sectioned in slide for Oil Red O staining. The immunohistostaining was performed according to instruction of the streptavidin-biotin complex (SABC) assay (Boster, China). Paraffin-embedded sections were dewaxed with xylene and rehydrated in series of alcohols, incubated at 95 °C for 5 min in antigen retrieval (0.01 M citrate buffered saline, pH 6.0) and then at room temperature for 20 min. The sections were then treated with 3% hydrogen peroxide for 5 min. The slides were treated with 5% bovine serum albumin (Boster, China) to prevent nonspecific antibody binding. The primary antibody treatment was done overnight at 4 °C in PBS. Imaging was obtained using a Nikon microscope and analyzed by software (HMIAS-2000, Champion Image Inc, China).

### 2.8. Statistical analysis

The data were analyzed by SPSS 20.0 statistical analysis software and results were expressed as the mean ± standard deviation (S.D.). The significant difference was statistically analyzed using Student's *t*-test in two groups. The significant difference was statistically analyzed using ANOVA in more than two groups. $P < 0.05$ (two tails) was considered statistically significant.

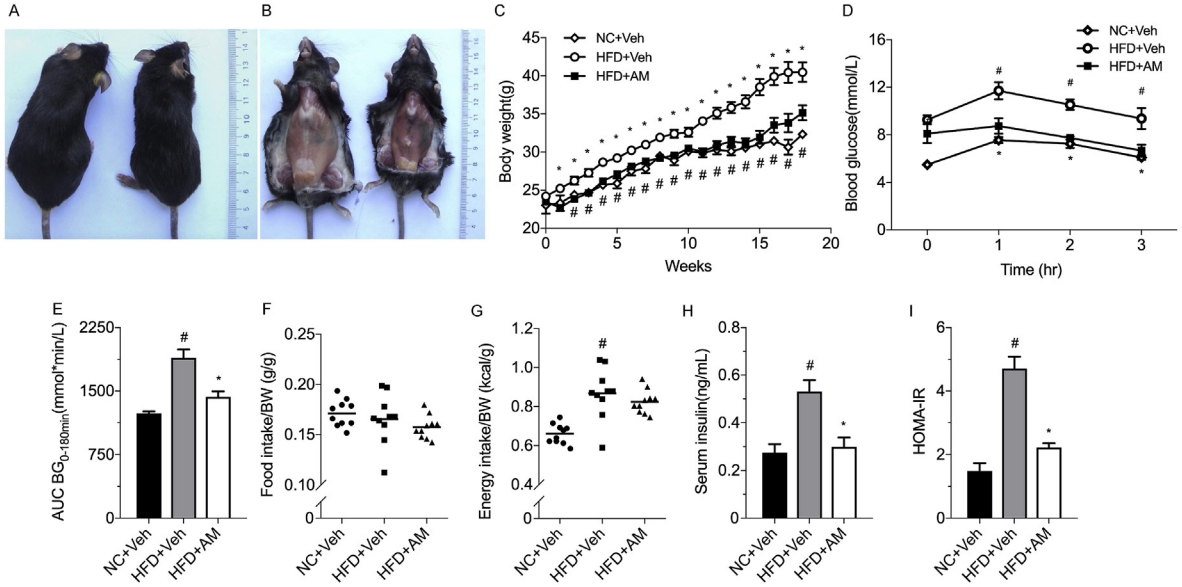


**Fig. 1. Amlexanox prevents weight gain and produces reversible metabolic changes in HFD-fed mice.** (A) Representative images of HFD-fed mice (left) and HFD-fed amlexanox-treated mice for 18 weeks (right). (B) Adipose tissue shown in representative images of HFD-fed mice (left) and HFD-fed amlexanox-treated mice (right). (C) Body weight in each group indicated. (D) Oral glucose tolerance test in the preventative treatment group. (E) Area under the curve (AUC) for OGTT (BG 0–180min) in each group. (F and G) Food intake or energy intake per gram body weight after 4 weeks treatment. (H) Fasting serum insulin (FINS) levels were detected by ELISA kit. (I) The homeostasis model assessment of insulin resistance (HOMA-IR) index was calculated according to [FBG (mmol/L) × FINS (mIU/L)]/ 22.5. n = 10 per group. $\#P < 0.05$ for NC (normal chow) + vehicle (Veh)-treated controls compared with HFD + Veh-treated controls, $*P < 0.05$ for HFD + Veh-treated controls compared with HFD + amlexanox-treated mice. All data in the figure are shown as the mean ± S.D. or as a dot plot showing each data point and the mean.

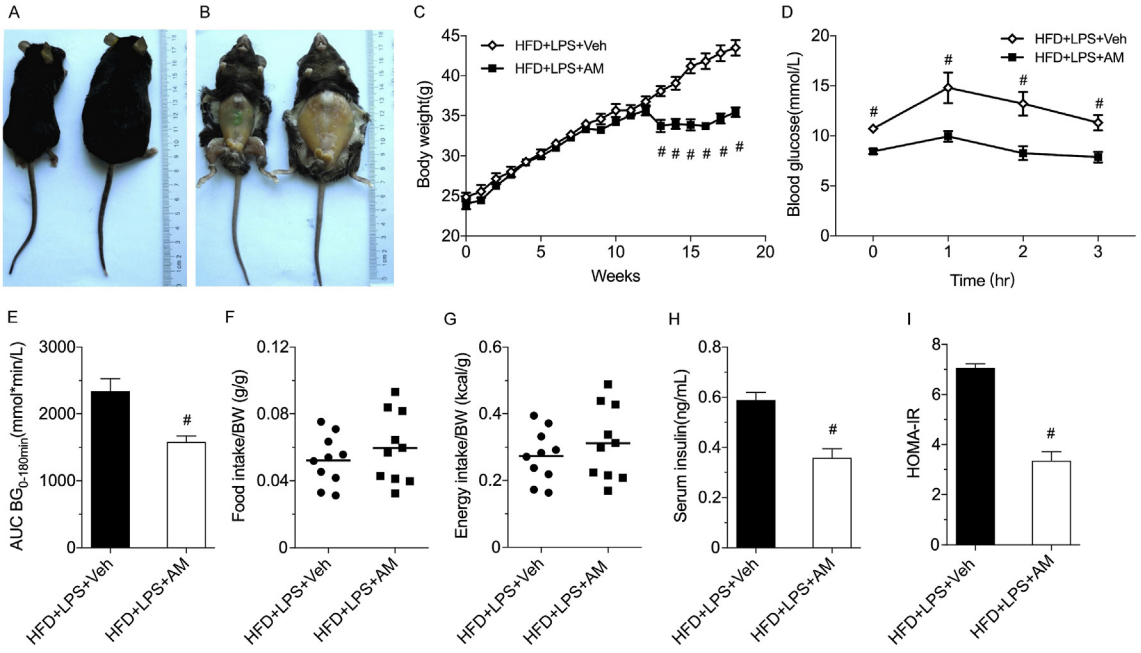


**Fig. 2. Amlexanox reverses weight gain and metabolic disorders in HFD + LPS induced mice.** (A) Representative images of mice induced by HFD + LPS (right) and HFD + LPS induced mice in which amlexanox was administrated by gavage for six weeks after week 12 (left). (B) Adipose tissue shown in representative images of HFD + LPS induced mice (right) and HFD + LPS induced amlexanox-treated mice (left). (C) Body weight of mice induced by HFD + LPS and mice in which amlexanox was administrated by gavage after week 12. (D) Oral glucose tolerance test (OGTT) in the treatment group. (E) Area under the curve (AUC) for OGTT (BG $_{0–180min}$) in each group. (F and G) Food intake or energy intake per gram body weight after 4 weeks treatment. (H and I) Fasting serum insulin (FINS) and the homeostasis model assessment of insulin resistance (HOMA-IR) index. n = 10 per group. $\#P < 0.05$ compared with HFD + LPS induced controls. All data in the figure are shown as the mean ± S.D. or as a dot plot showing each data point and the mean.

**Table 2**
Characteristics of the experimental animals after intervention study (Mean ± S.D.).

| Index | NC + Veh (n = 10) | HFD + Veh (n = 10) | HFD + AM (n = 10) | HFD + LPS + Veh (n = 10) | HFD + LPS + AM (n = 10) |
|---|---|---|---|---|---|
| TC (mmol/L) | 1.83 ± 0.39[a] | 4.54 ± 0.23 | 2.27 ± 0.38[a] | 4.84 ± 0.23 | 3.67 ± 0.40[b] |
| TG (mmol/L) | 0.59 ± 0.06[a] | 1.27 ± 0.05 | 0.74 ± 0.06[a] | 1.50 ± 0.12 | 1.08 ± 0.03[b] |
| ALT (IU/L) | 37.50 ± 4.50 | 37.63 ± 4.20 | 26.50 ± 3.23[a] | 51.50 ± 2.99 | 29.67 ± 5.17[b] |
| AST (IU/L) | 125.00 ± 13.00 | 133.00 ± 14.37 | 86.50 ± 5.86[a] | 171.50 ± 8.85 | 134.25 ± 6.06[b] |
| FFA (μmol/L) | 423.39 ± 60.48[a] | 862.87 ± 56.93 | 621.64 ± 76.23[a] | 1086.71 ± 90.25 | 747.65 ± 71.17[b] |
| Liver weight (g) | 1.17 ± 0.06[a] | 1.75 ± 0.13 | 1.32 ± 0.06[a] | 2.05 ± 0.10 | 1.47 ± 0.05[b] |
| Liver triglyceride (mmol/g) | 0.79 ± 0.13[a] | 1.48 ± 0.33 | 0.67 ± 0.06[a] | 2.41 ± 0.50 | 1.00 ± 0.10[b] |

[a] $P < 0.05$, compared with HFD + Veh.
[b] $P < 0.05$, compared with HFD + LPS + Veh.

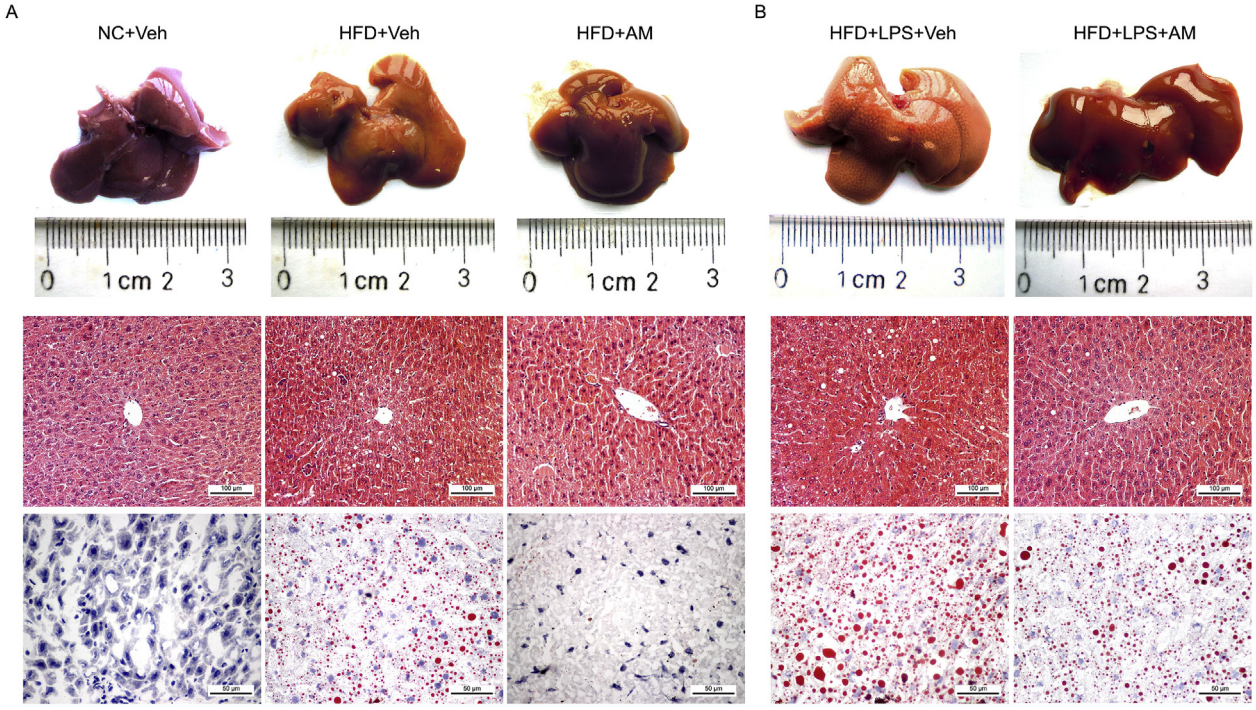


**Fig. 3. Amlexanox reverses hepatic steatosis in HFD-fed and HFD + LPS induced mice.** (A) Representative pictures of the livers of mice in HFD-fed mice gavaged with amlexanox (n = 10, right) or vehicle (n = 10, panels middle) and NC-fed mice (n = 10, left). Micrographs, H&E staining (20 × ) and Oil Red O staining of liver (40 × ) in the groups indicated. (B) Representative pictures of the livers of HFD + LPS induced mice (n = 10, left) and HFD + LPS induced amlexanox-treated mice (n = 10, right). Micrographs, H&E staining (20 × ) and Oil Red O staining of livers (40 × ) in the each group indicated.

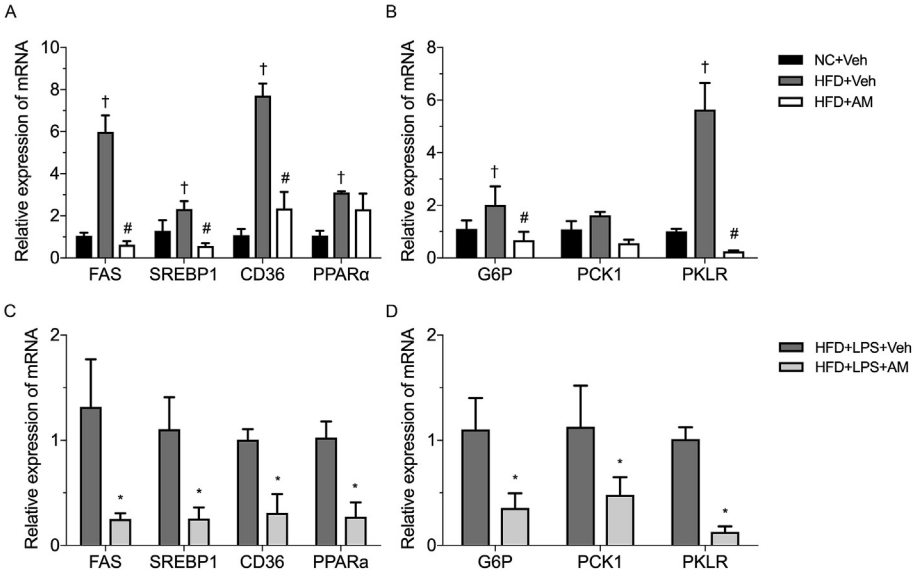


**Fig. 4. Amlexanox improves genes expression involved in glucose and lipid metabolism.** Expression of lipid metabolism genes (A and C) and glucose metabolism genes (B and D) in the livers of mice in each treatment group. The values are expressed as mean ± S.D., n = 6 independent experiments. #$P < 0.05$ compared with HFD-fed vehicle-treated control, +$P < 0.05$ compared with NC + Veh-treated controls, *$P < 0.05$ compared with HFD + LPS induced controls.

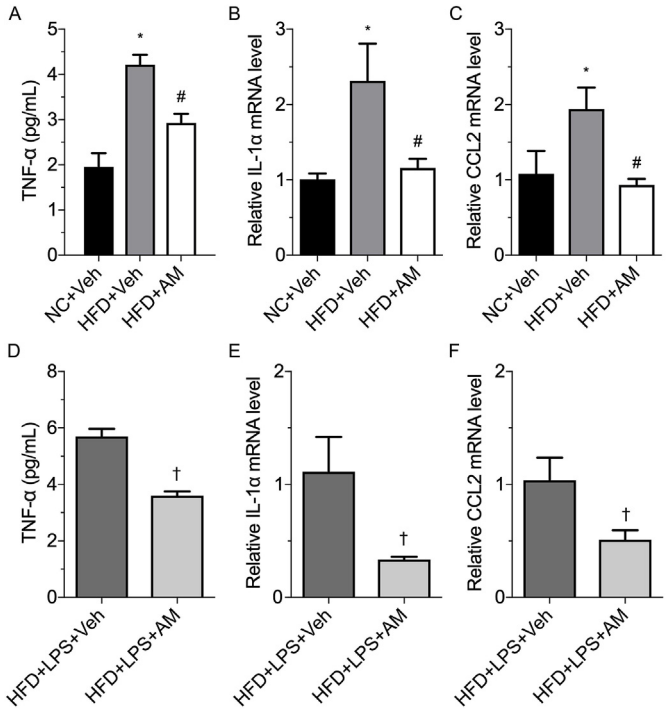


**Fig. 5. Amlexanox reduces liver inflammation in HFD-fed and HFD + LPS induced mice.** TNF-α levels (A and D) were detected by ELISA kit. The IL-1α (B and E) and CCL2 (C and F) mRNA levels were determined by quantitative real-time qRT-PCR in the groups indicated. The values are expressed as mean ± S.D. n = 6 independent experiments,. #$P < 0.05$ compared with HFD-fed vehicle-treated controls, *$P < 0.05$ compared with NC + Veh-treated controls, +$P < 0.05$ compared with HFD + LPS induced controls.

## 3. Results

### 3.1. Amlexanox produces reversible weight loss and metabolic changes in HFD-fed mice

The intervention A used oral administration to investigate the effect of amlexanox. Amlexanox prevented the weight gain produced by HFD (Fig. 1A–C) independent of influence on food intake and energy intake (Fig. 1F and G). Moreover, we assessed the metabolic parameters caused by amlexanox. Mice treated with amlexanox improved glucose tolerance especially postprandial glucose with an approximate 20% reduction in the area under the curve of OGTT (Fig. 1D and E). Amlexanox reversed the elevations in fasting serum insulin concentrations and HOMA-IR caused by the HFD, suggesting improved insulin sensitivity (Fig. 1H and I).

### 3.2. Amlexanox improves weight gain and metabolic disorders in HFD + LPS induced mice

In the intervention B, we evaluated amlexanox effect on HFD + LPS induced mice. Firstly, we displayed LPS increased lipid deposition even more significantly than HFD-fed mice, characterizing with moderate higher liver inflammation level and serum enzyme indexes (ALT, AST) through daily subcutaneous injection of LPS (Supplementary Fig). Secondly, HFD + LPS induced mice were treated with LPS for 12 weeks followed by amlexanox for 6 weeks. Amlexanox produced a 10 g weight loss (Fig. 2C) and fat mass decrease (Fig. 2A and B) in the absence of food intake or energy intake reduction (Fig. 2F and G). Mice treated with amlexanox significantly decreased blood glucose and the area under the curve of OGTT (Fig. 2D and E). Amlexanox showed similarly reversible effect in fasting serum insulin concentrations and HOMA-IR caused by HFD + LPS group (Fig. 2H and I). Totally, these findings showed amlexanox improved weight gain and metabolic disorders in two NAFLD models (HFD-fed mice and HFD + LPS induced mice).

### 3.3. Amlexanox reverses hepatic steatosis in HFD-fed and HFD + LPS induced mice

To further investigate the protective role of amlexanox in liver tissue in NAFLD, we evaluated morphologic characteristics and serum parameters. Serum triglyceride (TG), serum cholesterol (TC), serum free fatty acids (FFA), serum alanine aminotransferase (ALT), and aspartate transaminase (AST), which were elevated in HFD-fed mice, were reduced by amlexanox (Table 2). Larger lipid droplets in liver were shown in HFD-fed mice by H&E and Oil Red O staining, but were largely disseminated by treatment with amlexanox (Fig. 3A), which was consistent with marked reduction in liver weight and liver triglyceride content (Table 2). Similar phenotype was seen in HFD + LPS induced mice (Fig. 3B, Table 2). These data suggested that amlexanox lowered lipids accumulation in liver tissue in HFD-fed group and HFD + LPS group.

### 3.4. Amlexanox improves genes expression involved in glucose and lipid metabolism

Firstly, we examined expression of genes involved in lipid metabolism. To investigate lipogenic mechanism of amlexanox action, it was found that amlexanox decreased mRNA levels of FAS and SREBP1. Because SREBP1-FAS was important pathway in lipid synthesis, there indicated that amlexanox reduced lipid synthesis (Fig. 4A and C). PPARα is a key nuclear factor involved in lipid oxidation and CD36 plays an important role in the lipid entry into mitochondria. HFD was associated with compensatory high expression of PPARα and CD36 (Fig. 4A), indicating a higher lipid overload. PPARα and CD36 in liver tissue were decreased by amlexanox in HFD + LPS induced mice (Fig. 4C). CD36 was decreased while PPARα remained unchanged in HFD-fed mice by amlexanox (Fig. 4A).

Also, this assay checked gene expression involved in hepatic glucose metabolism. Gluconeogenic genes (G6P, PCK1) in liver tissue were decreased by amlexanox in HFD + LPS induced mice (Fig. 4D).This was improved by lower fasting blood glucose. G6P was decreased after amlexanox treatment in HFD-fed mice however PCK1 remained unchanged (Fig. 4B). Glycolytic gene (PKLR), which had higher expression in HFD-fed mice, was reversed to lower level in amlexanox-treated mice (Fig. 4B and D). These results suggested that amlexanox could decrease hepatic gluconeogenesis and lipid synthesis.

### 3.5. Amlexanox reduces liver inflammation in HFD-fed and HFD + LPS induced mice

The characteristic of non-alcoholic fatty liver disease is a low grade inflammation. Since LPS was a trigger of inflammatory cascade, we assessed inflammatory reactions. We found increased levels of pro-inflammatory genes (IL-1α, CCL2) and serum TNF-α in HFD-fed (Fig. 5A–C) and HFD + LPS induced mice (Fig. 5D–F). Interestingly, amlexanox improved serum concentration of TNF-α and pro-inflammatory genes expression both in HFD-fed and HFD + LPS induced mice (Fig. 5A–F).

### 3.6. Amlexanox reduces IKKε expression in hepatic stellate cell

We found IKKε was not expressed in hepatocytes, but in the liver interstitium. HFD could increase the expression of IKKε in liver interstitium (Fig. 6A), which was further raised by LPS treatment (Fig. 6B). IKKε expression was significantly decreased using amlexanox in HFD-fed and HFD + LPS induced mice (Fig. 6A and B). To figure out the positioning of IKKε, we used serial slices and conducted immunohistochemistry stain of IKKε and α-SMA, a marker of hepatic

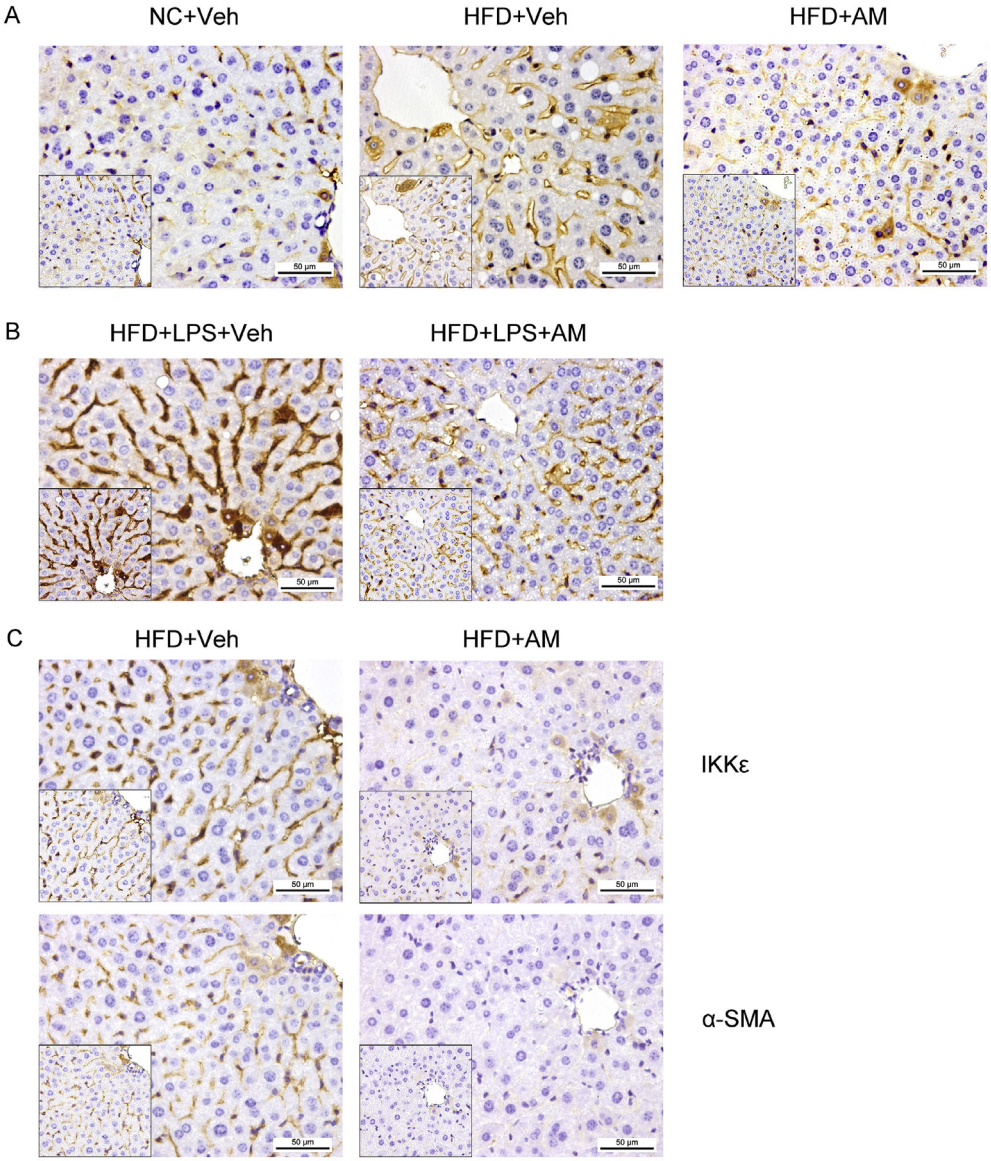


**Fig. 6. Immunohistochemical staining of IKKε or α-SMA.** (A and B) IKKε expression and location were assessed in groups indicated. (C) IKKε (top line) and α-SMA (bottom line) location were evaluated through immunohistochemical staining of serial sections in HFD + Veh group (left) and HFD + AM group (right). As α-SMA was a marker of hepatic stellate cells activation, amlexanox reduced IKKε expression in hepatic stellate cells. Representative micrographs are shown at 200-fold (left bottom) and 400-fold (right enlarge) magnification. n = 3 independent experiments.

stellate cells activation. Our results showed IKKε was precisely and specifically expressed in HSCs (Fig. 6C). However, amlexanox decreased IKKε and α-SMA expression in HSCs of HFD-fed mice, suggesting that amlexanox reduced activation of HSCs through inhibiting IKKε expression.

### *3.7. Amlexanox improves insulin signaling and inflammation pathway in liver tissue*

The expression of IKKε and the phosphorylation of NF-κB subunit (p65) were decreased by amlexanox in HFD-fed and HFD + LPS induced mice (Fig. 7A–D), however the phosphorylation of Akt and insulin receptor substrate-1 (IRS-1) were increased (Fig. 7E), as a key signal transduction molecule in insulin pathway. Considering decreased serum and gene levels of inflammatory markers (Fig. 5), the results showed amlexanox improved insulin signaling through inhibiting the inflammatory pathway mediated by NF-κB signaling.

## 4. Discussion

Non-alcoholic fatty liver disease is one of the most common liver diseases in adults and emerging as a new health crisis worldwide [17]. Through extensive previous researches, it has become clear that inflammation and insulin resistance are involved in the pathogenesis of NAFLD, involving multiple signaling pathways. NF-κB has a key role in the development in NAFLD [3]. Lipopolysaccharide (LPS) is the trigger of NF-κB pathway through toll-like receptor (TLR) and IKKε could also be inducible expressed. Many previous studies showed that both inflammatory stimuli (LPS) and diet-related metabolic challenge (carbohydrate, cholesterol) promoted the progression of NAFLD [18,19]. Nevertheless, they often used continuous subcutaneous infusion of LPS. In this study, we displayed HFD + LPS increased lipid deposition even more significantly than HFD-fed mice, suggesting LPS led to NASH through NF-κB signaling, which established stable NASH model and subcutaneous injection (once daily, 125 μg/kg) was recommended procedure to aggravate lipid deposition which was used in following assay.

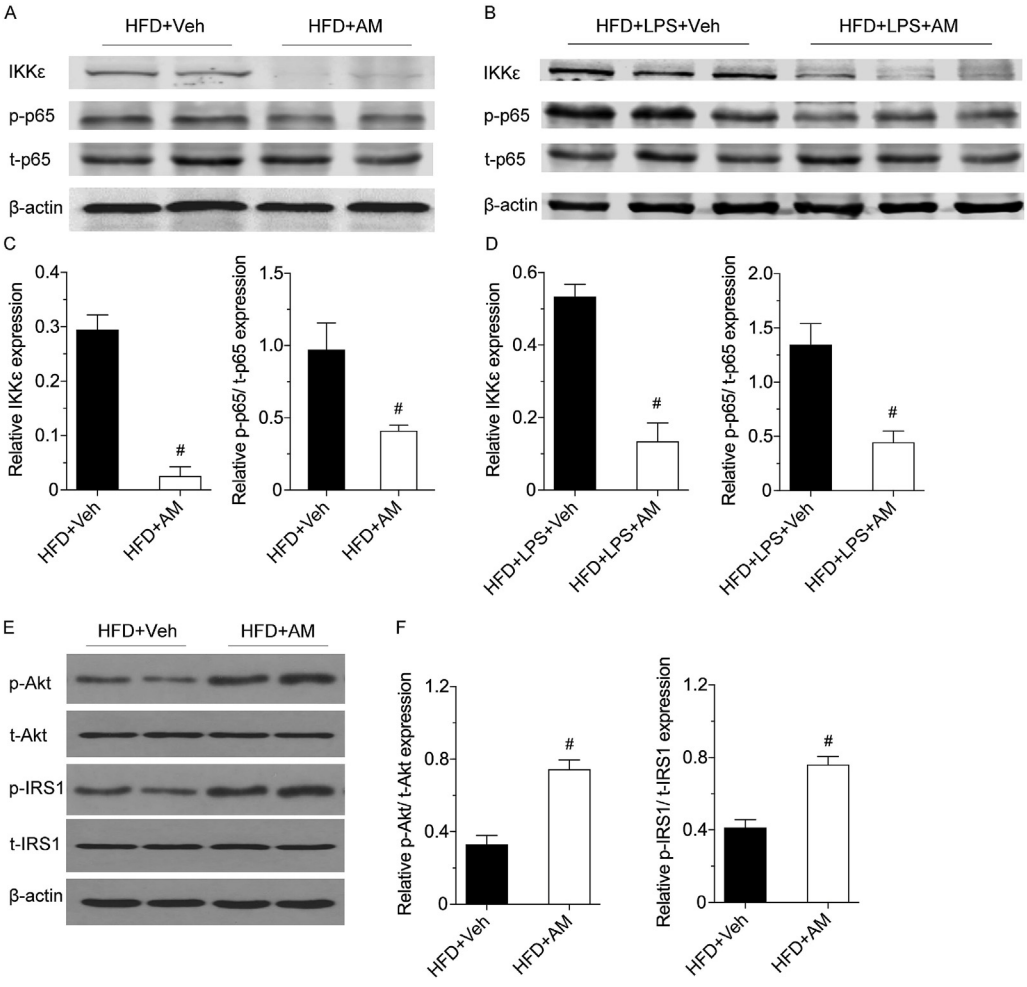


**Fig. 7. Amlexanox improves insulin signaling and inflammation pathway in liver tissue.** (A) The expression levels of IKKε, p65 and phosphorylated p65 (p-p65) were examined by western blotting in HFD-fed mice and HFD-fed amlexanox-treated mice. (B) The expression levels of IKKε, p65 and p-p65 in HFD + LPS induced mice and HFD + LPS induced amlexanox-treated mice. (C and D) Statistical analyses of brand intensity of IKKε and p-p65/t-p65 in groups were presented. (E) The expression levels of Akt, phosphorylated Akt (p-Akt), IRS1 and p-IRS1 in HFD-fed mice and HFD-fed amlexanox-treated mice. (F) Statistical analyses of brand intensity of p-Akt/t-Akt and p-IRS1/t-IRS1. n = 5 independent experiments. #*P* < 0.05 compared with HFD + Veh -treated or HFD + LPS induced controls.

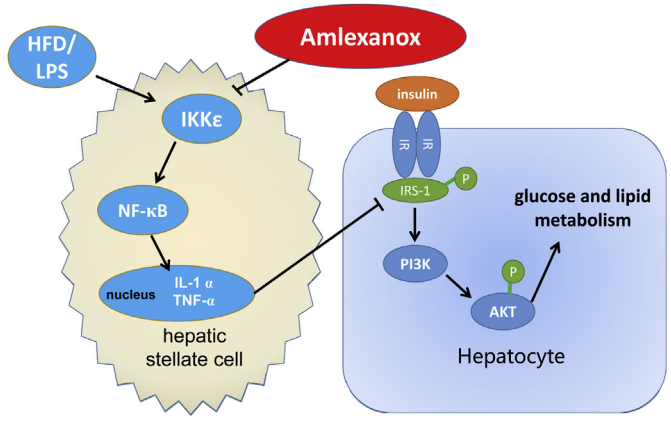


**Fig. 8. Schematic model of altered insulin pathway in hepatocyte by amlexanox effect on hepatic stellate cell.** Amlexanox inhibited IKKε expression in HSC cells, which led to a reduction in inflammation factors secreted by HSCs then insulin signaling pathway (Insulin-IR-IRS-1-Akt) were increased. Furthermore insulin signaling pathway related genes were altered, including hepatic gluconeogenesis (G6P, PCK1) and lipid synthesis (SREBP1-FAS).

IKKε, one of the noncanonical IKKs, also named inducible IKK (IKKi), has been reported to have significant roles in liver steatosis [8], obesity [20], osteoclast-related disorders [21] and cancer [22]. Furthermore, suppression of the IKKε has been proved to restore insulin sensitivity [8] and promote regeneration of pancreatic β-cells [23]. TBK1 had highly homologous structure with IKKε. TBK1 deficiency also impaired activation and nuclear translocation of interferon β (IFNβ) regulatory factor-3 (IRF3) which led to IFNβ production in response to virus infection. Previous studies have showed its role on antiviral innate immune responses [24] and oncogenic role in melanoma [25], non-small cell lung cancer (NSCLC) [26], HTLV-1 (human T-cell leukemia virus type 1) [27], and breast cancer [28]. Few studies showed its role in metabolic diseases. TBK1 is ubiquitously expressed in all tissues, whereas IKKε expression only in specific tissues, with highest levels found in lymphoid tissues, peripheral blood lymphocytes and the pancreas, including moderate physiological expression in liver tissue [29–31]. But it is unknown where IKKε is expressed in liver. Recent researches showed HFD led to a sustained elevation of IKKε in liver, adipocytes, and adipose tissue macrophages (ATMs) [8,12]. In this study, we firstly reported that IKKε was not expressed in hepatocytes but in liver interstitium in normal chow diet group, and inducibly expressed in hepatocytes and HSCs of HFD and HFD + LPS induced groups. Intriguingly, amlexanox significantly decreased IKKε expression in liver (both HSCs and hepatocytes) in all groups above. Moreover, we conducted serial liver slices, immunohistochemistry of IKKε/α-SMA and found that IKKε and α-SMC was co-expressed in HSCs.

As a small molecular and dual inhibitor of IKKε and TBK1, amlexanox has been reported of anti-inflammatory, anti-allergic, anti-tumor [32], immunomodulation activity, and it is ever used to treat recurrent aphthous ulcers (now still used in China), allergic rhinitis and asthma [33,34]. Its mechanism of action might involve inhibition of inflammation by reducing the release of histamine and leukotrienes. A subset of amlexanox responders in a placebo-controlled study of 42 obese patients exhibited improvements in insulin sensitivity and hepatic steatosis, following a transient increase in serum IL-6 level [35].

In our study, we showed that amlexanox produced reversible weight loss, improved metabolic disorders and attenuated hepatic steatosis even in non-alcoholic steatohepatitis induced by HFD + LPS. Furthermore, we explored the underlying mechanism of its protective role and found amlexanox showed increased Akt and IRS1 phosphorylating, suggesting enhanced insulin signaling. However, previous studies proposed that IKKs could activate Akt by directly phosphorylating Akt on Thr308 and Ser473 on HeLa cell in vitro study [36], which seems to be controversial with our findings. Recent reports indicated amlexanox restored insulin sensitivity in obese mice. Nevertheless, the compound was not direct insulin sensitizers in vitro [12]. Moreover, recent study revealed the mechanism of insulin-sensitizing effects of amlexanox including the secretion of cytokine IL-6 from adipocytes in the subcutaneous adipose tissue resulted in the over-activation of hepatic STAT3, which suppressed expression of G6P to reduce hepatic glucose output [37]. Thus, we hypothesized amlexanox increased phosphorylating of Akt and IRS1 through indirect mechanism. In this study, we found amlexanox reduced IKKε expression in liver nonparenchymal cells and defined it HSC as high expression of smooth muscle actin-α (α-SMA) through serial slices immunohistochemistry.

HSCs are one of the inherent liver nonparenchymal cell types located in the Disse space. Studies have revealed that there is paracrine mechanism in the liver under the accumulation of free cholesterol (FC) accumulation [38]. Activation of nonparenchymal cells caused the secretion of pro-inflammatory mediators (e.g. IL-6, 8 and TNF-α) that influenced neighboring cells and induced inflammation [38,39]. These changes resulted in HSC activation and increased liver fibrosis. Finally, FC accumulation in hepatocytes induced itself lipid peroxidation and lipotoxicity leading to cellular dysfunction and death. These events led to a vicious circle that caused progressive liver damage, inflammation, and steatosis which ultimately led to the progression to NASH. Recent research also indicated that chemokine CCL5 was one of the HSC-secreted mediators and directly induced downstream pro-inflammatory factors in healthy hepatocytes through the receptor CCR5 [40]. In this study, we found IKKε and NF-κB in HSCs were inhibited by amlexanox and pro-inflammatory factors IL-1α and TNF-α reduced, suggesting amlexanox affected hepatocytes by paracrine. The amlexanox reduced liver inflammation and reversed hepatic steatosis. Furthermore, amlexanox increased phosphorylating of Akt and IRS1 suggesting suppressed insulin signaling by pro-inflammatory factors altered which reversed glucose and lipid metabolism disorders.

In summary, the study suggested that inhibition of activation in HSCs was responsible for the metabolic activities of amlexanox (Fig. 8). Amlexanox reduced the activation of NF-κB in HSC and resulted in downstream downregulated synthesis of pro-inflammatory mediators (e.g. IL-1α and TNF-α), which reduced liver inflammation. It was supposed that decreased HSC-secreted pro-inflammatory mediators attenuated insulin resistance in hepatocytes through paracrine mechanism, which was altered by amlexanox action. Improved insulin signaling caused gene changes in glucose and lipid metabolism.

## 5. Conclusion

In conclusion, the present study confirmed the protective effects of amlexanox on non-alcoholic fatty liver disease models and provided evidence that amlexanox indirectly enhanced insulin signaling in hepatocytes through inhibiting inflammation in hepatic stellate cells, resulting in improvement in glucose and lipid metabolism in liver. Considering our current results and the proven pharmacologic safety of amlexanox in mice, we believe it might be worthwhile to re-purpose amlexanox for non-alcoholic fatty liver disease.

## Authors' contribution is as following

X.Z., X.X., Q.H. contributed to the experiment design; Q.H., X.X., K.Y., J.Z., W.W., Q.W., R.T. contributed to the acquisition and analysis of data; X.X. reviewed the manuscript; X.Z., X.X. obtained the funding; and Q.H., X.X. and X.Z. wrote the manuscript.

## Declaration of competing interest

The authors declare no conflicts of interest.

## Acknowledgements

This work was supported by grants from Scientific Research Project of Health Commission of Hubei Province (WJ2019M064), Medical and Health Research Project of Yichang (A19-301-17) and Young Scientist foundation of Hubei Health and Family Planning Commission (WJ2015Q036).

## Appendix A. Supplementary data

Supplementary data to this article can be found online at https://doi.org/10.1016/j.lfs.2019.117010.

## References

[1] A.J. Sanyal, Past, present and future perspectives in nonalcoholic fatty liver disease, Nat. Rev. Gastroenterol. Hepatol. 16 (2019) 377–386.
[2] V.T. Samuel, Z.X. Liu, X. Qu, B.D. Elder, S. Bilz, D. Befroy, et al., Mechanism of hepatic insulin resistance in non-alcoholic fatty liver disease, J. Biol. Chem. 279 (2004) 32345–32353.
[3] M.C. Arkan, A.L. Hevener, F.R. Greten, S. Maeda, Z.W. Li, J.M. Long, et al., IKK-beta links inflammation to obesity-induced insulin resistance, Nat. Med. 11 (2005) 191–198.
[4] K.E. Wellen, G.S. Hotamisligil, Inflammation, stress, and diabetes, J. Clin. Investig. 115 (2005) 1111–1119.
[5] M. Yuan, N. Konstantopoulos, J. Lee, L. Hansen, Z.W. Li, M. Karin, et al., Reversal of obesity- and diet-induced insulin resistance with salicylates or targeted disruption of Ikkbeta, Science 293 (2001) 1673–1677.
[6] M. Corr, D.L. Boyle, L. Ronacher, N. Flores, G.S. Firestein, Synergistic benefit in inflammatory arthritis by targeting I kappaB kinase epsilon and interferon beta, Ann. Rheum. Dis. 68 (2009) 257–263.
[7] K. Bulek, C. Liu, S. Swaidani, L. Wang, R.C. Page, M.F. Gulen, et al., The inducible kinase IKKi is required for IL-17-dependent signaling associated with neutrophilia and pulmonary inflammation, Nat. Immunol. 12 (2011) 844–852.
[8] S.H. Chiang, M. Bazuine, C.N. Lumeng, L.M. Geletka, J. Mowers, N.M. White, et al., The protein kinase IKKepsilon regulates energy balance in obese mice, Cell 138 (2009) 961–975.
[9] T. Saijo, H. Kuriki, Y. Ashida, H. Makino, Y. Maki, Mechanism of the action of amoxanox (AA-673), an orally active antiallergic agent, Int. Arch. Allergy Appl. Immunol. 78 (1985) 43–50.
[10] D.D. Darshan, C.N. Kumar, A.D. Kumar, N.S. Manikantan, D. Balakrishnan, M.P. Uthkal, Clinical study to know the efficacy of Amlexanox 5% with other topical Antiseptic, Analgesic and Anesthetic agents in treating minor RAS, J. Int. Oral Health 6 (2014) 5–11.
[11] R. Sharma, S. Pallagatti, A. Aggarwal, S. Sheikh, R. Singh, D. Gupta, A randomized, double-blind, placebo-controlled trial on clinical efficacy of topical agents in reducing pain and frequency of recurrent aphthous ulcers, Open Dent. J. 12 (2018) 700–713.
[12] S.M. Reilly, S.H. Chiang, S.J. Decker, L. Chang, M. Uhm, M.J. Larsen, et al., An inhibitor of the protein kinases TBK1 and IKK-varepsilon improves obesity-related metabolic dysfunctions in mice, Nat. Med. 19 (2013) 313–321.
[13] S.L. Friedman, Hepatic stellate cells: protean, multifunctional, and enigmatic cells of the liver, Physiol. Rev. 88 (2008) 125–172.
[14] E. Seki, R.F. Schwabe, Hepatic inflammation and fibrosis: functional links and key pathways, Hepatology 61 (2015) 1066–1079.
[15] T. Tsuchida, S.L. Friedman, Mechanisms of hepatic stellate cell activation, Nat. Rev. Gastroenterol. Hepatol. 14 (2017) 397–411.
[16] J.C. McGrath, E. Lilley, Implementing guidelines on reporting research using animals (ARRIVE etc.): new requirements for publication in BJP, Br. J. Pharmacol. 172 (2015) 3189–3193.
[17] K. Hassan, V. Bhalla, M.E. El Regal, A.K. HH, Nonalcoholic fatty liver disease: a comprehensive review of a growing epidemic, World J. Gastroenterol. 20 (2014) 12082–12101.
[18] W. Liang, J.H. Lindeman, A.L. Menke, D.P. Koonen, M. Morrison, L.M. Havekes, et al., Metabolically induced liver inflammation leads to NASH and differs from LPS- or IL-1beta-induced chronic inflammation, Lab. Investig. 94 (2014) 491–502.
[19] P.D. Cani, J. Amar, M.A. Iglesias, M. Poggi, C. Knauf, D. Bastelica, et al., Metabolic endotoxemia initiates obesity and insulin resistance, Diabetes 56 (2007) 1761–1772.
[20] L. Scheja, B. Heese, K. Seedorf, Beneficial effects of IKKepsilon-deficiency on body weight and insulin sensitivity are lost in high fat diet-induced obesity in mice, Biochem. Biophys. Res. Commun. 407 (2011) 288–294.

[21] Y. Zhang, H. Guan, J. Li, Z. Fang, W. Chen, F. Li, Amlexanox suppresses osteoclastogenesis and prevents ovariectomy-induced bone loss, Sci. Rep. 5 (2015) 13575.
[22] H. Li, L. Chen, A. Zhang, G. Wang, L. Han, K. Yu, et al., Silencing of IKKepsilon using siRNA inhibits proliferation and invasion of glioma cells in vitro and in vivo, Int. J. Oncol. 41 (2012) 169–178.
[23] J. Xu, Y.F. Jia, S. Tapadar, J.D. Weaver, I.O. Raji, D.J. Pithadia, et al., Inhibition of TBK1/IKKepsilon promotes regeneration of pancreatic beta-cells, Sci. Rep. 8 (2018) 15587.
[24] S.M. McWhirter, K.A. Fitzgerald, J. Rosains, D.C. Rowe, D.T. Golenbock, T. Maniatis, IFN-regulatory factor 3-dependent gene expression is defective in Tbk1-deficient mouse embryonic fibroblasts, Proc. Natl. Acad. Sci. U. S. A 101 (2004) 233–238.
[25] B. Eskiocak, E.A. McMillan, S. Mendiratta, R.K. Kollipara, H. Zhang, C.G. Humphries, et al., Biomarker accessible and chemically addressable mechanistic subtypes of BRAF melanoma, Cancer Discov. 7 (2017) 832–851.
[26] J.M. Cooper, Y.H. Ou, E.A. McMillan, R.M. Vaden, A. Zaman, B.O. Bodemann, et al., TBK1 provides context-selective support of the activated AKT/mTOR pathway in lung cancer, Cancer Res. 77 (2017) 5077–5094.
[27] H. Zhang, L. Chen, S.H. Cai, H. Cheng, Identification of TBK1 and IKKepsilon, the non-canonical IkappaB kinases, as crucial pro-survival factors in HTLV-1-transformed T lymphocytes, Leuk. Res. 46 (2016) 37–44.
[28] C. Wei, Y. Cao, X. Yang, Z. Zheng, K. Guan, Q. Wang, et al., Elevated expression of TANK-binding kinase 1 enhances tamoxifen resistance in breast cancer, Proc. Natl. Acad. Sci. U. S. A 111 (2014) 601–610.
[29] T. Shimada, T. Kawai, K. Takeda, M. Matsumoto, J. Inoue, Y. Tatsumi, et al., IKK-i, a novel lipopolysaccharide-inducible kinase that is related to IkappaB kinases, Int. Immunol. 11 (1999) 1357–1362.
[30] Y. Tojima, A. Fujimoto, M. Delhase, Y. Chen, S. Hatakeyama, K. Nakayama, et al., NAK is an IkappaB kinase-activating kinase, Nature 404 (2000) 778–782.
[31] C.H. Shin, D.S. Choi, Essential roles for the non-canonical IkappaB kinases in linking inflammation to cancer, obesity, and diabetes, Cells 8 (2019) 178.
[32] Y. Liu, J. Lu, Z. Zhang, L. Zhu, S. Dong, G. Guo, et al., Amlexanox, a selective inhibitor of IKBKE, generates anti-tumoral effects by disrupting the Hippo pathway in human glioblastoma cell lines, Cell Death Dis. 8 (2017) e3022.
[33] J. Bell, Amlexanox for the treatment of recurrent aphthous ulcers, Clin. Drug Investig. 25 (2005) 555–566.
[34] H. Makino, T. Saijo, Y. Ashida, H. Kuriki, Y. Maki, Mechanism of action of an antiallergic agent, amlexanox (AA-673), in inhibiting histamine release from mast cells. Acceleration of cAMP generation and inhibition of phosphodiesterase, Int. Arch. Allergy Appl. Immunol. 82 (1987) 66–71.
[35] E.A. Oral, S.M. Reilly, A.V. Gomez, R. Meral, L. Butz, N. Ajluni, et al., Inhibition of IKKvarepsilon and TBK1 improves glucose control in a subset of patients with type 2 diabetes, Cell Metabol. 26 (2017) 157–170.
[36] X. Xie, D. Zhang, B. Zhao, M.K. Lu, M. You, G. Condorelli, et al., IkappaB kinase epsilon and TANK-binding kinase 1 activate AKT by direct phosphorylation, Proc. Natl. Acad. Sci. U. S. A 108 (2011) 6474–6479.
[37] S.M. Reilly, M. Ahmadian, B.F. Zamarron, L. Chang, M. Uhm, B. Poirier, et al., A subcutaneous adipose tissue-liver signalling axis controls hepatic gluconeogenesis, Nat. Commun. 6 (2015) 6047.
[38] G. Arguello, E. Balboa, M. Arrese, S. Zanlungo, Recent insights on the role of cholesterol in non-alcoholic fatty liver disease, Biochim. Biophys. Acta 1852 (2015) 1765–1778.
[39] A. Leroux, G. Ferrere, V. Godie, F. Cailleux, M.L. Renoud, F. Gaudin, et al., Toxic lipids stored by Kupffer cells correlates with their pro-inflammatory phenotype at an early stage of steatohepatitis, J. Hepatol. 57 (2012) 141–149.
[40] B.M. Kim, A.M. Abdelfattah, R. Vasan, B.C. Fuchs, M.Y. Choi, Hepatic stellate cells secrete Ccl5 to induce hepatocyte steatosis, Sci. Rep. 8 (2018) 7499.